

# Discrete Multiwavelet Transform Based SAR Image Speckle Reduction

Sujit Bhattacharya\*, V. R. Gujaraty and S. S. Rana

Microwave Sensors Group, Space Applications Center  
Indian Space Research Organization (ISRO)  
Ambawadi Vistar P.O. Ahmedabad – 380 015  
Gujarat, India

E-mail: \*sujit@sac.ernet.in

## ABSTRACT

Speckle noise usually occurs in Synthetic Aperture Radar (SAR) images owing to coherent processing of SAR data. This paper proposes and investigates the Speckle reduction and enhancement of SAR images with multiple wavelets (Multiwavelets). Multiwavelets transformations are useful for speckle reduction through its sub-band images and the speckle reduction is obtained by thresholding the sub-band images coefficients of the digitized SAR images. Generalized Cross Validation (GCV) based thresholding of the Multiwavelet sub-band coefficients for the logarithmically transformed SAR image data is investigated. The GCV technique has proven to be an effective statistical way for estimating the optimum threshold required for denoising. Assuming that observations within a SAR images are outcome of independent Rayleigh random variables, the proposed method shows a good performance regarding signal-to-noise ratio improvement and edge preservation criteria. The algorithms have been applied to various simulated and actual SAR images.

**Keywords:** SAR, speckle, multiwavelets, thresholding, GCV.

## 1. INTRODUCTION

Synthetic Aperture Radar (SAR) is an active coherent all weather imaging system that operates in the microwave region (1.25-35.3 GHz) (wavelength=24-0.8cm) of the spectrum. It can penetrate foliage and clouds and operate day or night because it provides its own illumination. The main problem with the use of SAR images is a kind of signal-dependent noise: the *speckle noise*. When an object is illuminated by a coherent source and the object has a surface structure that is roughly of the order of a wavelength of the incident radiation, the wave reflected from such a surface consists of contributions from many independent scattering points. Interference of these de-phased but coherent waves result in the granular pattern known as *speckle*. Thus, speckle tends to obscure image details as it produces salt-pepper effect and hence speckle reduction is important in most detection and recognition system.

It can be shown and verified that speckle has the characteristics of a random multiplicative noise [1] in that

the noise level (or standard deviation) increases with the magnitude of the radar back scattering (or the mean). The Additive White Guassian Noise (AWGN) model is a good approximation for speckle [2] when considering the SAR intensity/magnitude image (e.g. the dB image). Logarithmic transformation of a SAR image converts the multiplicative noise model to an additive noise model.

The effect of speckle in SAR images can be reduced by two techniques. The first is the sub-aperture (multi-look) processing applied during the image formation and the second is the image domain filtering technique. The former improves the SAR image by averaging the uncorrelated images from non-overlapping spectrum. The latter tries to suppress speckle noise after the image has been formed. Most image domain filters suppress speckle noise utilizing the spatial correlation between pixels. Speckle noise filters include mean filter, Frost filter, Lee filter, Kuan/ Nathan filter, etc [3]. In speckled radar images, filtering must achieve a tradeoff between smoothing of homogeneous area and edge and texture preservation. In this work, information processing has been carried out in (multi) wavelet domain.

Donoho and Johnstone [4] pioneered the theoretical formalization of filtering additive *i.i.d.* Guassian noise (of zero mean and standard deviation  $\sigma$ ) via thresholding wavelet coefficients. A wavelet coefficient is compared to a given threshold and is set to zero if its magnitude is less than the threshold; otherwise, it is kept or modified (depending upon the thresholding rule). The threshold acts as an *oracle*, which distinguishes between the insignificant coefficients likely due to noise, and the significant coefficients consisting of important signal structures. For image denoising, the threshold choice proposed by Dohono [5] yield overly smoothed images as the threshold choice of  $\sigma\sqrt{2\log M}$  (called the universal threshold), can be unwarrantedly large due to its dependence on the number of samples,  $M$ , which is more than  $10^5$  for a typical test image of size 512 x 512. This thresholding mechanism also requires the knowledge of amount of noise present in the image. It has been proved that the minimum of the "Generalized Cross Validation" is an asymptotically optimal threshold [6].

Wavelet transform [7] performs a hierarchical decomposition of the signal space into a nested sequence of approximation spaces by translations and dilatations of one mother wavelet function. Whereas, the Multiwavelets spans

the ‘‘lowpass’’ space by translations and dilations of more than one mother wavelet functions [8]. They are known to have several advantages over scalar wavelets such as support, orthogonality, symmetry, and higher order vanishing moments. Strela *et al.* [9] claimed that multiwavelet soft thresholding offer better results than the traditional scalar wavelet soft thresholding. Since the wavelet thresholding have been applied to log transformed SAR images for speckle reduction [10], it is natural to attempt multiwavelet denoising. GCV based thresholding method has been used for denoising and their results with various multiwavelets are compared. Classical measures of speckle (evaluated on homogeneous region) are the standard-deviation-to-mean (std/m) ratio and log standard deviation (log-std) [2]., both of which should decrease as a result of speckle reduction.

The rest of the paper is organized as follows. Section 2 first presents a brief introduction to multiwavelets. One major difference between single and multiple wavelets is that the data have to be preprocessed before applying the discrete wavelet transform. Section 3 discusses various preprocessing filters used. Section 4 discusses the speckle reduction by thresholding of multiwavelet coefficients. The algorithm for SAR image speckle reduction is described in Section 5. Section 6 presents some experimental results, followed by the conclusions in Section 7.

## 2. DISCRETE MULTIWAVELETS TRANSFORM

The wavelets are based on the idea of multiresolution analysis (MRA). In wavelet it is usually assumed that MRA is generated by one scaling function and dilates and translates of only one wavelet  $\Psi \in L^2(\mathfrak{R})$  form a stable basis of  $L^2(\mathfrak{R})$ . Generalizing the wavelet case, one can allow a multiresolution analysis  $\{V_n\}_{n \in \mathbb{Z}}$  of  $L^2(\mathfrak{R})$  to be generated by a finite number of scaling functions  $\mathbf{f}_1, \mathbf{f}_2, \dots, \mathbf{f}_r$  and their integer translates (the multiresolution analysis is then said to be of *multiplicity*  $r$ ). A vector function  $\Phi := (\mathbf{f}_1, \dots, \mathbf{f}_r)^T$  where  $r$  is a fixed positive integer and  $\mathbf{f}_j, j = 1, 2, \dots, r$ , are compactly supported functions in  $L^2(\mathfrak{R})$ , is called an *orthogonal multiscaling function* if it satisfies the refinement equation

$$\Phi(x) = \sum_{k \in \mathbb{Z}} H_k \Phi(2x - k), \quad (1)$$

where  $H_k$  is a finitely supported sequence of  $r \times r$  matrices, and

$$\langle \mathbf{f}_i(\cdot - k), \mathbf{f}_j(\cdot - l) \rangle = \mathbf{d}_{i,j} \mathbf{d}_{k,l},$$

for  $k, l \in \mathbb{Z}, i, j = 1, \dots, r$ . Let  $V_0$  be a closed linear span of the integer shifts of  $\mathbf{f}_j$ , i.e.,

$$V_0 = \overline{\text{span}\{\mathbf{f}_j(x - k) : k \in \mathbb{Z}, j = 1, 2, \dots, r\}},$$

and  $V_u = \{g \in L^2(\mathfrak{R}) : g(2^{-u} \cdot) \in V_0\}$ . Then we have i)  $V_u \subset V_{u+1}$ , ii)  $\bigcap_{u \in \mathbb{Z}} V_u = \{0\}$ , and iii)  $\bigcup_{u \in \mathbb{Z}} V_u$  is dense in

$L^2(\mathfrak{R})$ . In other words,  $(V_u)$  generates a multiresolution analysis (MRA) of  $L^2(\mathfrak{R})$  of multiplicity  $r$ .

Further, let  $W_0 \perp V_0$  be the orthogonal complement of  $V_0$  in  $V_1$ . If  $\mathbf{y}_j \in W_0, j = 1, 2, \dots, r$ , and their integer shifts  $\mathbf{y}_j(\cdot - k), k \in \mathbb{Z}, j = 1, 2, \dots, r$ , constitute an orthonormal basis of  $W_0$ , then  $\mathbf{y}_j, j = 1, 2, \dots, r$ , are called orthogonal *multiwavelets* associated with  $\Phi$ . We shall also call the vector function  $\Psi = (\mathbf{y}_1, \dots, \mathbf{y}_r)^T$  a multiwavelet. Since  $W_0 \subset V_1, \Psi$  satisfies

$$\Psi(x) = \sum_{k \in \mathbb{Z}} G_k \Phi(2x - k), \quad (2)$$

for some finitely supported sequence of  $r \times r$  matrices  $G_k$ . Equivalently, in the Fourier domain, the refinement equation (1) can be written as

$$\hat{\Phi}(2\mathbf{w}) = \hat{H}(\mathbf{w}) \hat{\Phi}(\mathbf{w}), \quad \text{for all } \mathbf{w} \in \mathbb{R},$$

where  $\hat{H}(\mathbf{w}) = \frac{1}{2} \sum_{k \in \mathbb{Z}} H_k e^{-ik\mathbf{w}}$  is the *matrix lowpass frequency response* associated with  $\Phi$ . Similarly, we have  $\hat{G}(\mathbf{w}) = \frac{1}{2} \sum_{k \in \mathbb{Z}} G_k e^{-ik\mathbf{w}}$  as the corresponding *matrix highpass frequency response*. In addition, if the following orthogonal perfect reconstruction criterion is satisfied

$$\begin{pmatrix} \hat{H}(\mathbf{w}) & \hat{H}(\mathbf{w} + \mathbf{p}) \\ \hat{G}(\mathbf{w}) & \hat{G}(\mathbf{w} + \mathbf{p}) \end{pmatrix} \begin{pmatrix} \hat{H}(\mathbf{w}) & \hat{H}(\mathbf{w} + \mathbf{p}) \\ \hat{G}(\mathbf{w}) & \hat{G}(\mathbf{w} + \mathbf{p}) \end{pmatrix}^* = I_{2rx2r},$$

where the superscript  $*$  denotes conjugate transpose, then  $\{H_k, G_k\}$  is said to constitute a *perfect reconstruction orthogonal multiwavelet system* of multiplicity  $r$  (for a more rigorous theoretical treatment of multiwavelets refer to [8]). A particular signal of interest,  $f(x) \in V_0$ , can be written as a linear combination of the basis functions  $\{\mathbf{f}_m(x - k)\}_{m=1,2,\dots,r}$ , with weight vector  $v_{0,k} = [v_{0,k}^1 v_{0,k}^2 \dots v_{0,k}^r]^T$ :

$$f(x) = \sum_{k=-\infty}^{\infty} v_{0,k}^T \Phi(x - k) = \sum_{k=-\infty}^{\infty} \sum_{l=1}^r v_{0,k}^l \mathbf{f}_l(x - k)$$

where

$$v_{0,k}^l = \int_{-\infty}^{\infty} f(x) \mathbf{f}_l(x - k) dx$$

In the scalar-valued expression  $v_{j,k}^l$ ,  $j$  refers to the scale,  $k$  refers to the translation, and  $l$  refers to the sub-channel or vector row.

The filter bank implementation equation becomes:

$$v_{j,k} = \sum_{m=-\infty}^{\infty} H_{m-2k} v_{j+1,m} \quad (3)$$

$$w_{j,k} = \sum_{m=-\infty}^{\infty} G_{m-2k} v_{j+1,m} \quad (4)$$

This is one stage of a multi-input multi-output (MIMO) filter bank as shown in Figure 1. The reconstruction formula for orthogonal multiscaling and multiwavelet functions takes the form

$$v_{j+1,k} = \sum_{m=-\infty}^{\infty} H_{k-2m}^T v_{j,m} + \sum_{m=-\infty}^{\infty} G_{k-2m}^T w_{j,m} \quad (5)$$

which is the synthesis equation.

### Multiscaling and Wavelet functions

In practice multiscaling and wavelet functions are concerned with multiplicity  $r = 2$ . In this paper we use the multiwavelet constructed by Geronimo, Hardin and Massopust [11], which we shall refer to as GHM system.

The GHM scaling functions have short support, has second order approximation, the translates of the scaling functions are orthogonal and both scaling functions and the wavelets are symmetric.

The Chui and Lian's (CL4) and SA4 multiwavelet belong to the class of multifilters for which the scaling and wavelet functions are symmetric/antisymmetric pairs [12]. The CL4 multiwavelet has the highest possible approximation order of 3 for its filter length.

The analytical part of DMWT can be implemented as a level transformation or two channel matrix filter bank. The two input data streams are lowpass ( $H_k$ ) and highpass ( $G_k$ ) filtered and downsampled by 2. At the next level the two output lowpass data streams from the previous level are again lowpass and highpass filtered and downsampled by 2. In order to start this cascade algorithm one must preprocess the original scalar data to get vector input. This preprocessing or prefiltering is going to be investigated in the next section. For image data each level of the DMWT is performed on the rows of preprocessed image data and then on its columns.

### 3. PREPROCESSING OR PREFILTERING

One of the main challenges to the application of multiwavelets is the problem of *multiwavelet initialization* (or better known as *pre-filtering* in the literature). In the case of scalar wavelets, the given signal data is usually assumed to be the scaling coefficients that are sampled at a certain resolution, and hence, we can directly apply multiresolution decomposition on the given signal. Unfortunately, the same technique cannot be employed directly in the multiwavelet setting. Some processing has to be performed on the input signal prior to multiwavelet decomposition.

The main idea of pre-filtering is to obtain the multiple (vector) input streams  $v_{0,k}$  from a given scalar input signal  $f_k$ , so that the vector streams can be operated on by the matrix filters. This preprocessing is a linear operator that maps  $f_k$  to the starting coefficients  $v_{0,k}$ . This operator usually takes the form of a filter and hence the operation is often called prefiltering. In our case  $r = 2$  and the two data streams enter the multifilter. If the scalar data is of length  $N$  and the prefiltering produces  $N, 2 \times 1$  vectors it is said to be an *oversampling* scheme. On the other hand, if the prefiltering produces  $N/2, 2 \times 1$  vectors the result is a

*critical sampling* scheme. In critical sampling case a prefilter partitions the data into a sequence of 2 vectors and applies the filter  $Q$ , which is defined by a sequence of  $2 \times 2$  matrices  $Q_n$ .

Thus,

$$v_{0,k} = \sum_n Q_n \begin{bmatrix} f_{2(n+k)} \\ f_{2(n+k)+1} \end{bmatrix}$$

To recover the signal after reconstruction the output coefficients have to be postprocessed. The postfilter  $P$  that accompanies the prefilter  $Q$  satisfies  $PQ = I$  where  $I$  is the identity filter. So, if one applies a prefilter, DMWT, inverse DMWT and postfilter to any sequence the output will be identical to the input. The various prefilters GHMInter, CLInter, Haar, Oversampling considered are given in [12].

### 4. SPECKLE REDUCTION THROUGH THRESHOLDING OF MULTIWAVELETS COEFFICIENTS

As discussed in the previous section, the *speckle* noise typically can be modeled as a multiplicative *i.i.d.* Gaussian noise. Logarithmic transformation of a SAR image converts the multiplicative noise model to an additive noise model. For a digitized SAR image, we define  $y(j,k)$  as the gray level (the observed image magnitude) of the  $(j,k)$  th pixel of the image. Hence, the pixel level of a SAR image can be written as

$$y = xe$$

where  $x$  is the desired radiometric information, and  $e$  is the multiplicative speckle noise. For logarithmically transformed SAR image, the speckle is approximately Gaussian additive noise, i.e.,

$$\tilde{y} = \tilde{x} + \tilde{e} \text{ where } \tilde{y} = \ln(|y|).$$

In what follows  $\tilde{y}$  will represent a logarithmically transformed gray level (or intensity),  $y$ . If  $W$  is the multilevel DMWT, then a multiresolution representation is given by the equation

$$W\tilde{y} = W\tilde{x} + W\tilde{e} \text{ or } w = v + \mathbf{v}$$

where  $w = W\tilde{y}$ ,  $v = W\tilde{x}$ , and  $\mathbf{v} = W\tilde{e}$

The standard deviation of the noise in the multiresolution representation  $\mathbf{s}$  is not known in advance and must be estimated from the data.

To reduce the contribution of the smallest coefficients that contain mainly noise, a soft threshold [5] is applied to all the wavelet coefficients except those of the lowest scale. A soft threshold operation involves choosing a threshold  $I$ , and applying the function

$$f(w) = \text{sign}(w)(|w| - I)_+ \quad (6)$$

to obtain the enhanced subband DMWT coefficients,  $\hat{w}$ . Finally, the speckle-reduced image is obtained from the synthesis part of the DMWT of the enhanced subband image  $f(w)$ .

The central issue in a threshold procedure is the selection of an appropriate threshold. If this threshold is too small, the result is still noisy. On the other hand, a large threshold also removes important image features and thus causes a bias. The optimal threshold for subband  $j$ ,  $I_{j,opt}$  minimizes the mean square error of the result as compared with the unknown, noise free coefficients:

$$R_j(I) = \frac{1}{N_j} \|w_{j,I} - v_j\|^2$$

where  $N_j$  is the number of coefficients in the subband  $j$ ,  $w_{j,I}$  is the vector of threshold noisy coefficients and  $v_j$  is the vector of noise-free coefficients. As threshold value, we use the minimizer of the ‘‘Generalized Cross Validation’’ (GCV) function

$$GCV_j(I) = \frac{\frac{1}{N_j} \|w_j - w_{j,I}\|^2}{\left[ \frac{N_{j0}}{N_j} \right]^2} \quad (7)$$

where  $N_{j0}$  is the number of wavelet coefficients that were replaced by zero. This procedure does not need an estimate of the actual noise level,  $s_j$ .

## 5. THE ALGORITHM

The thresholding method of SAR image using DMWT can now be described using the following steps

1. Logarithmically transform the SAR image i.e. compute the intensity SAR image.
2. First pre-process all rows, then all columns of the row-pre-processed data by a specific prefilter.
3. Perform the 2D DMWT, by tensor product of two 1D DMWT, to level  $J$ . During each level the multiwavelet filter bank is applied first to the rows and then to the column of the low/low output from the previous step.
4. Compute the threshold value for each sub-band through GCV function using equation (7).
5. Apply soft thresholding to the DMWT coefficients obtained in step 3 using equation (6). No thresholding is performed on the low/low output of level  $J$ .
6. Perform the inverse DMWT and exponential operation in order to acquire the final SAR image with an improvement in its radiometric quality.

## 6. EXPERIMENTAL RESULTS

To demonstrate the efficacy of the proposed method for speckle noise removal, we have tested the algorithm with two different cases. First, we use a simulated speckle image

and then we applied the algorithm to a single look 256 x 256, 256-gray-scale SAR

The simulated image as shown in Figure 2(a), contains two regions of intensity 150 and 200 on a background of intensity 80. The original image is multiplied by the Gaussian distributed random variable with mean 1 and variance 0.068, shown in Figure 2(b). We used GHM, CL4 and SA4 with appropriate prefilters as described in the previous section. The matrix filter coefficients for each multiwavelet system were used in a 3-level ( $J = 3$ ) DMWT. Filtered images are shown in Figure 2(c) and (d).

The multiwavelet coefficients are threshold with a threshold value computed for each subband (except of LL subband) and sub-levels through GCV method. A typical GCV curve is shown in Figure 5.

Table 1 gives the value of the standard-deviation-to-mean ratio values of the simulated image and SAR image. The low values of (std/m) and (log-std) indicates better speckle reduction.

Figure 3(a) and (b) represent one of the scan lines of the simulated image. The data was extracted from the 65<sup>th</sup> column to the 220<sup>th</sup> column at the 150<sup>th</sup> row of the image.

## 7. CONCLUSIONS

In this paper, we discussed the implementation of the Generalized Cross Validation (GCV) technique based thresholding of the Multiwavelet coefficients for the logarithmically transformed SAR image for speckle reduction. The algorithm suppresses the speckle noise in the homogeneous region and preserves the fine details such as edges and textures. Experimental results are encouraging and further work with Translation Invariant (TI) multiwavelets for SAR speckle reduction is envisaged.

**Acknowledgement:** The principal author would like to thank Prof. K.R. Ramakrishnan, Department of Electrical Engg., IISc, Bangalore, for kind support and guidance to carry out this work. Deep-hearted gratitude remains with Prof. Vittal Rao, Department of Mathematics, IISc, Bangalore, for building up the strong mathematical foundation required for wavelet theory.

## 8. REFERENCES

- [1] J. S. Lee, ‘‘Speckle analysis and smoothing of synthetic aperture radar images’’, *Computer Graphics Image Processing*, 16(4), pp. 24-32, 1981.
- [2] J. W. Goodman, ‘‘Some fundamental properties of speckle’’, *J. Opt. Soc. Am.*, 66:pp-1145-1150, Nov 1976.
- [3] E. Herve, R. Fjortoft, P. Marthon and A. Lopes, ‘‘Comparison of Wavelet-based and Statistical Speckle Filters,’’ *EUROPTO Conference on SAR Image Analysis, Modeling, and Techniques*. Barcelona, Spain, Sep. 1998.
- [4] D. L. Donoho, and I. M. Johnstone, ‘‘Ideal spatial adaptation via wavelet shrinkage,’’ *Biometrika*, 81, pp. 425-455, 1994.
- [5] D. L. Donoho, ‘‘Denoising by soft-thresholding,’’ *IEEE Transaction on Information Theory*, 41(3), pp. 613-627, May. 1995.
- [6] M. Jansen, M. Malfait and A. Bultheel, ‘‘Generalized cross-validation for wavelet thresholding,’’ *Signal Processing*, 56(1), pp. 33-44, Jan 1997.
- [7] S. G. Mallat, ‘‘A theory of multiresolution signal decomposition: The wavelet representation,’’ *IEEE Transactions on Pattern Analysis and Machine Intelligence*, 11(7): pp. 674-693, Jul. 1989.
- [8] T. N. T. Goodman and S. L. Lee, ‘‘Wavelets of multiplicity  $r$ ,’’ *Trans. Amer. Math. Soc.*, 342, pp. 373-401, 1994.



[9] V. Strela, P. N. Heller, G. Strang, P. topiwala, and C. Heil, "The application of multiwavelet filter banks to image processing," *IEEE Trans. Image Processing*. Vol.8.pp.548-562, April,1999.

[10] H. Guo, J. E. Odegard, M. Lang, R.A. Gopinath, et al., "Wavelet based speckle reduction with application to SAR

based ATD/R," *Proc. IEEE Int. Conf. Image Processing*, volume 1, pp. 75-79, Austin, TX, Nov 1994.

[11] J. Geronimo, D. Hardin, and P. Massopust. "Fractal Functions and wavelet expansions based on several scaling functions," *J. Approx. Theory*, 78:pp. 373-401, 1994.

[12] T. R. Drownie, "Signal Processing in Multiwavelets", *preprint* 1998.

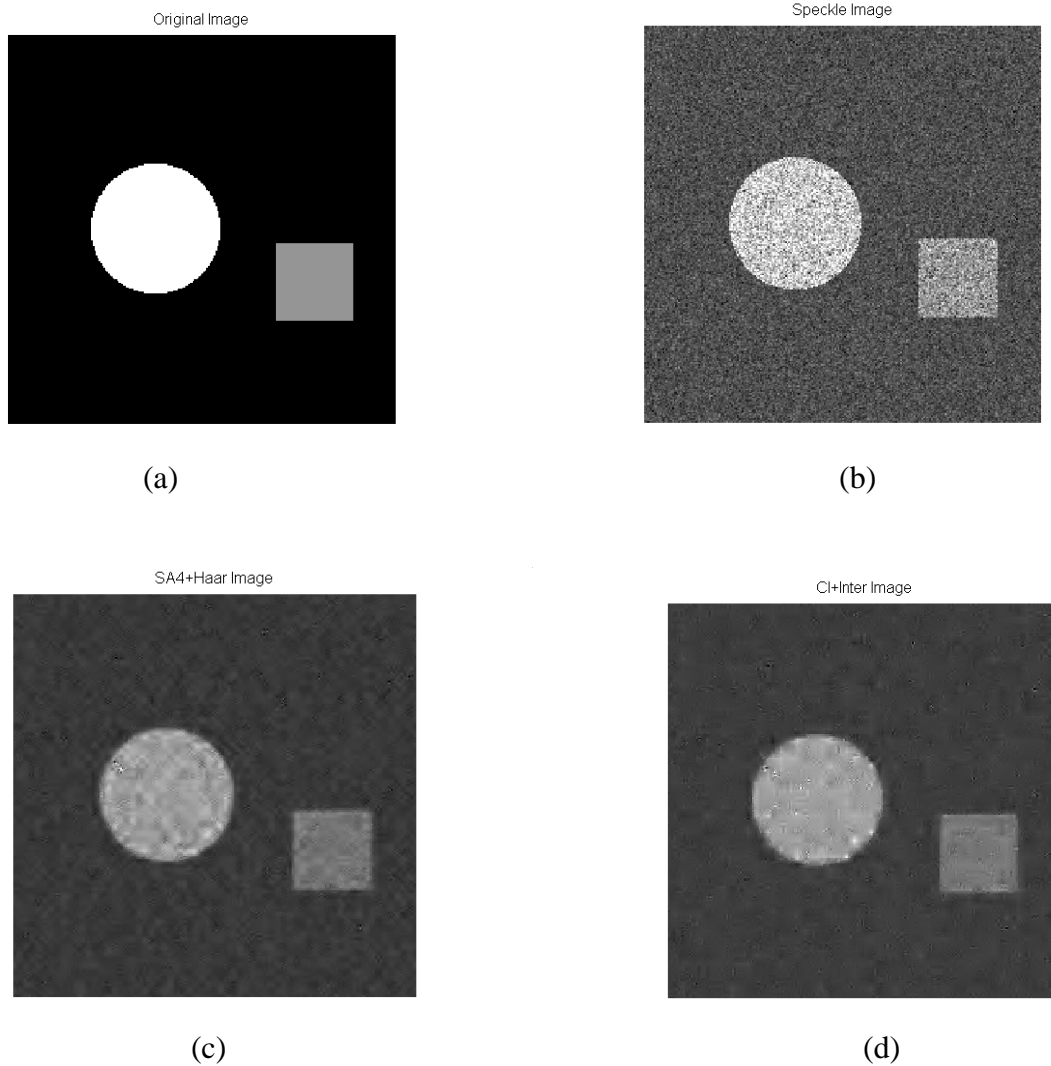


Fig 2. Simulated Test Image. a) Original Image containing two regions of intensity 150 and 200 on a background of intensity 80. b) Speckled Image by multiplicative noise with  $\text{var}=0.068$  c) Processed Image with SA4+Haar d) Processed Image with CL+Inter

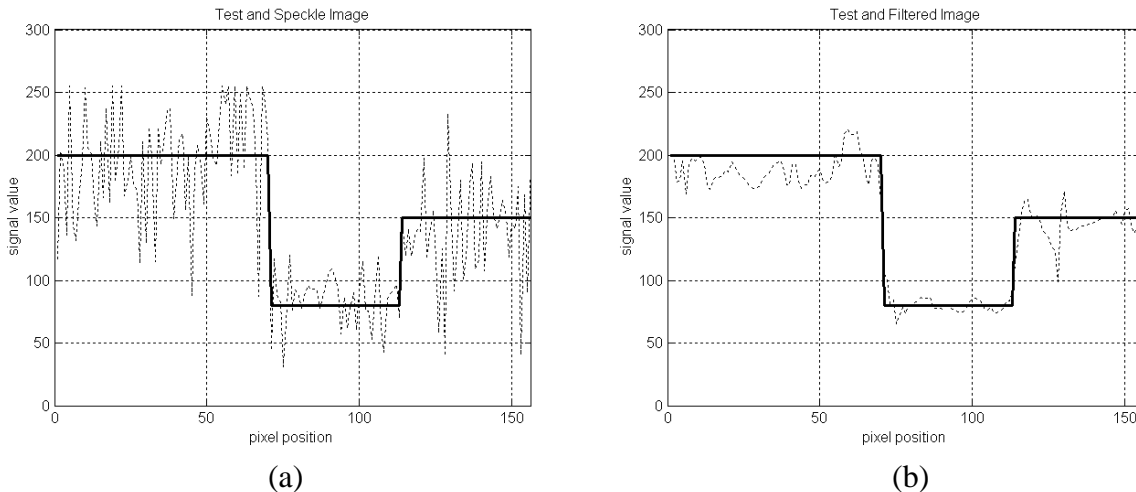


Fig 3. One-dimensional data of Test Image. a) Original Image and Speckled Signal extracted from 150<sup>th</sup> row b) Original Image and Processed Image with SA4+Haar

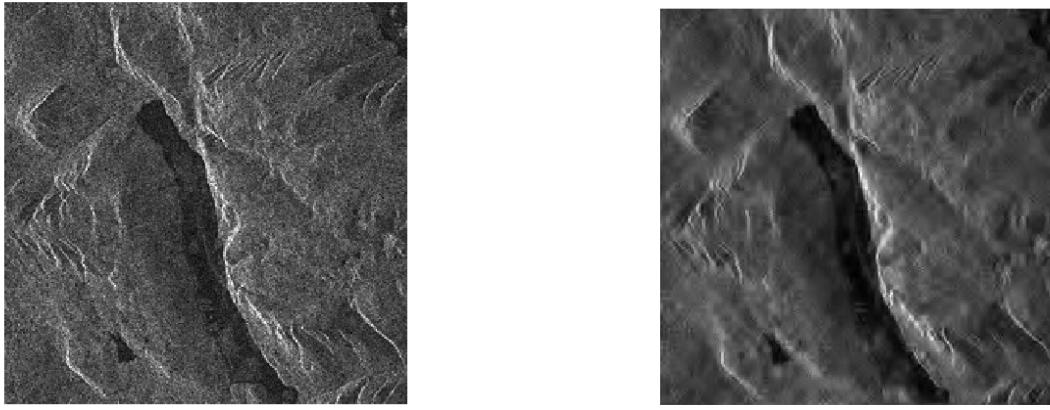


Fig 4. SAR Image. a) Original Image containing speckle. b) Processed Image with SA4+Haar

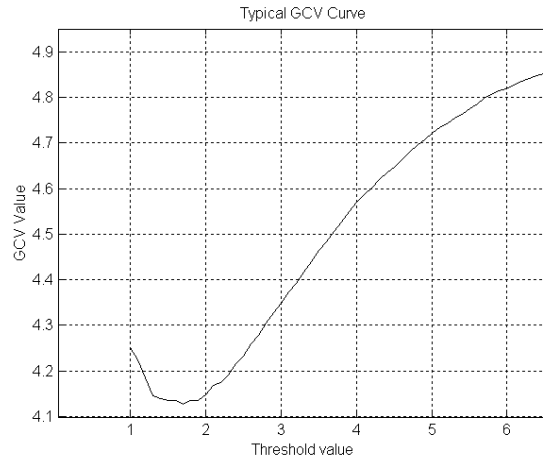


Fig 5. Typical GCV Curve of a sub-band of Multiwavelet Transform

<b>Simulated Image</b>	<b>std_dev/mean ratio</b>	<b>Log(std_dev) (dB)</b>
Original Image	0.259	38.99
GHM+GHMInter	0.122	17.38
CL+CLInter	0.081	11.50
SA4+Haar	0.086	12.35
GHM+RR	0.113	16.12
CI+RR	0.096	13.78
<b>SAR Image</b>	<b>std_dev/mean ratio</b>	<b>Log(std_dev) (dB)</b>
Original Image	0.200	19.66
GHM+GHMInter	0.092	8.86
CL+CLInter	0.073	7.01
SA4+Haar	0.088	8.50
GHM+RR	0.103	10.02
CI+RR	0.102	9.91

Table 1. Standard deviation to mean ratio and log standard deviation of Simulated and SAR Images